34th Annual International Conference of the IEEE EMBS
San Diego, California USA, 28 August - 1 September, 2012

An Ultra-Sensitive Wearable Accelerometer for Continuous Heart and Lung Sound Monitoring

Yating Hu and Yong Xu, *Member, IEEE*

Abstract— **This paper presents a chest-worn accelerometer with high sensitivity for continuous cardio-respiratory sound monitoring. The accelerometer is based on an asymmetrical gapped cantilever which is composed of a bottom mechanical layer and a top piezoelectric layer separated by a gap. This novel structure helps to increase the sensitivity by orders of magnitude compared with conventional cantilever based accelerometers. The prototype with a resonant frequency of 1100Hz and a total weight of 5 gram is designed, constructed and characterized. The size of the prototype sensor is 35mm×18mm×7.8mm (*l*×*w*×*t*). A built-in charge amplifier is used to amplify the output voltage of the sensor. A sensitivity of 86V/g and a noise floor of 40ng/√Hz are obtained. Preliminary tests for recording both cardiac and respiratory signals are carried out on human body and the new sensor exhibits better performance compared with a high-end electronic stethoscope.**

I. Introduction

The cardio-respiratory signal is one of the fundamental vital signs to assess a person's health. Auscultation of the chest wall sounds which include both heart and lung sounds is a traditional and effective way to capture and diagnose many cardiovascular and respiratory diseases. The current solution for auscultation is the stethoscope, which is based on a bell-shaped air chamber to pick up and amplify sound signals. Although widely used in intermittent auscultation, the stethoscope has a number of limitations that prevent it from monitoring heart/lung sound continuously. For instance, it is difficult to be body-worn due to its bulky size. Furthermore, to record the signals, the stethoscope typically needs to be held against the skin by hands. This will lead to friction noise and make the detection of weak acoustic signals, such as lung sounds, very challenging.

Another approach of detecting heart/lung sounds is based on the accelerometer. Compared with the stethoscope, the miniaturized accelerometer can be taped on the chest wall for a more convenient and continuous cardio-respiratory monitoring. However, because it is in direct contact with the skin and does not have an air chamber to couple and amplify the acoustic signal, the accelerometer itself needs to have a very high sensitivity. There have been many efforts in the development of accelerometer based acoustic sensors for heart/lung sound monitoring [1-3]. Some researchers have used off-the-shelf accelerometers to detect heart/lung sounds. However, these off-the-shelf sensors are either too bulky or not sensitive enough to capture the details of heart sounds, let alone lung sounds. In this paper, we present an accelerometer based acoustic sensor with a high sensitivity for continuous cardio-respiratory sound monitoring. This sensor is based on a novel asymmetrical gapped cantilever structure which is composed of a bottom mechanical layer and a top piezoelectric layer separated by a gap. The sensitivity can be increased significantly by the asymmetrical gapped structure. From the energy perspective, the majority of mechanical energy can be concentrated on the piezoelectric layer. The overall energy conversion efficiency can reach about 90% for asymmetrical gapped cantilevers and only below 39% for conventional cantilevers. A prototype with a resonant frequency of 1100Hz is designed, constructed, and characterized. The size of the prototype sensor is 35mm×18mm×7.8mm (l×w×t). With a built-in charge amplifier, a sensitivity of 86V/g and a resolution of 40ng/√Hz are obtained. Preliminarily tests for recording both cardiac and respiratory signal are carried out on human body and demonstrate the superior performance of the new sensor over commercial stethoscope.

*Resrach partially supported by National Science Foundation under Grant No. 0747620. Any opinions, findings, and conclusions or recommendations expressed in this material are those of the author(s) and do not necessarily reflect the views of the National Science Foundation.

Y. Hu is with Department of Electrical and Computer Engineering, Wayne State University, Detroit, MI 48202 USA (e-mail: eb2256@wayne.edu).

Y. Xu is with Department of Electrical and Computer Engineering, Wayne State University, Detroit, MI 48202 USA (phone: 313-577-3850; fax: 313-577-1101; e-mail: yxu@eng.wayne.edu).

II. Sensor Design

Fig. 1(a) shows the basic structure of a conventional accelerometer: a proof mass suspended by one cantilever beam. A piezoelectric layer is integrated on the surface of the cantilever beam. Fig. 1(b) shows the schematic structure of the accelerometer based on asymmetrical gapped cantilever. It comprises a top piezoelectric beam ($w_2 \times t_2 \times l_2$), a bottom mechanical beam ($w_1 \times t_1 \times l_1$) and a proof mass or lever ($w_{pm} \times t_{pm} \times l_{pm}$). The distance between middle planes of top and bottom layers is *D*.

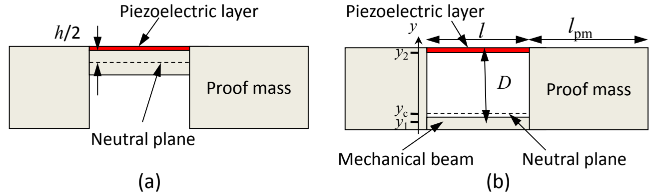

Figure 1. Comparison of the (a) conventional accelerometer (h is the cantilever thickness) and (b) new accelerometer design based on decoupled piezoelectric layer (asymmetric gapped cantilever).

It is worth noting that the deformation of the asymmetrically-gapped cantilever can be decomposed into pure bending (rotational movement) and S-shaping modes (translational movement) as shown in Fig. 2. Since the plane assumption is not valid in this case, conventional Euler-Bernoulli beam theory cannot be applied here. New analytical model has been developed for the asymmetrical gapped cantilever [4-6].

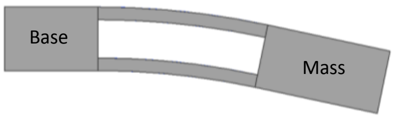

(a) Pure bending (rotational movement)

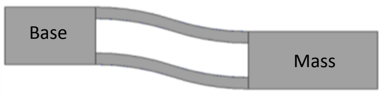

(b) S-shape bending (translational movement)

Figure 2. Two deformation modes of the asymmetrically-gapped cantilever.

The effective neutral plane of the asymmetrical gapped cantilever for pure bending mode is

$$y_{\mathrm{c}} = \frac{E_1 w_1 t_1 y_1 + E_2 w_2 t_2 y_2}{E_1 w_1 t_1 + E_2 w_2 t_2} \tag{1}$$

where y_1 and y_2 are the vertical positions (please refer to Fig. 1 (b)), E_1 and E_2 are Young's moduli of the bottom and top beams, respectively. The bending rigidities for pure bending and S-shape bending R_{P} and R_{S} are given by

$$R_{\mathrm{P}} = E_1\left(\frac{w_1 t_1^3}{12} + (y_1 - y_c)^2 w_1 t_1\right) + E_2\left(\frac{w_2 t_2^3}{12} + (y_2 - y_c)^2 w_2 t_2\right) \tag{2}$$

$$R_{\mathrm{S}} = E_1 \frac{w_1 t_1^3}{12} + E_2 \frac{w_2 t_2^3}{12} \tag{3}$$

The spring constants of the two modes are:

$$k_P = \frac{4R_S}{l^3}\frac{1}{\alpha^2\beta} \quad \text{and} \quad k_S = \frac{12R_S}{l^3} \qquad (4) \text{ and } (5)$$

where $\alpha = (l+l_{\mathrm{pm}})/l$ and $\beta = R_{\mathrm{S}}/R_{\mathrm{P}}$. Then, the total effective spring constant can be expressed as

$$k_{\mathrm{E}} = \left(\frac{1}{k_{\mathrm{P}}} + \frac{1}{k_{\mathrm{S}}}\right)^{-1} = \frac{12R_{\mathrm{S}}}{l^3}\frac{1}{3\alpha^2\beta + 1} \tag{6}$$

Based on Rayleigh-Ritz method [7], the resonant frequency is

$$f_0{}' = \frac{1}{2\pi}\sqrt{\frac{R_S}{ml^3}\frac{12(3\alpha^2\beta+1)}{(3\alpha^2\beta+1)^2 + 3\alpha^2\beta^2(\alpha-1)^2}} \tag{7}$$

The normal strain experienced by the top piezoelectric beam is:

$$\varepsilon_2 = \frac{ma(l + l_{\mathrm{pm}})(y_2 - y_{\mathrm{c}})}{2R_{\mathrm{P}}} \tag{8}$$

where a is the acceleration applied. It can be clearly observed that the sensitivity is proportional to y_2-y_{c}, the distance between the top piezoelectric beam and the neutral plane of the asymmetrical gapped cantilever. This distance is approximately equal to the height of the gap for asymmetrical gapped cantilevers. In comparison, for the conventional cantilever, this distance is only about half of the cantilever thickness (h/2) as shown in the Fig. 1 (a). If the the spring constants of the two designs are the same, the sensitivity of the new design will be $D/(h/2)$ times of the conventional cantilever. Since D can be much larger than h/2, the sensitivity of the new design will be orders of magnitude higher than the conventional one.

The advantage of the new structure can also be explained from the energy perspective [4-5]. Namely, it is desirable to allocate as much energy as possible for strain sensing from the total energy applied. Note that the vibration energy is distributed in different parts of the asymmetric gapped cantilever with different forms. However, what is effective in generating output voltage is only the energy stored in the top sensing layer in the form of normal strain. Here we defined the energy efficiency η as the ratio of the energy stored by normal strain of the top sensing layer to the total mechanical energy, which can be calculated in two steps. First, the ratio of the pure-bending energy to the total energy can be calculated from spring constants, which is

$$\eta_1 = \frac{k_S}{k_P + k_S} = \frac{1}{1/3\alpha^2\beta + 1} \tag{9}$$

The pure bending energy is further distributed in both top and bottom beams. The percentage of pure bending energy stored in the top sensing layer in the form of normal stain is

$$\eta_2 = \frac{E_2 w_2 t_2 (y_2 - y_{\mathrm{c}})^2}{R_{\mathrm{P}}} = (1-\beta)(1-\gamma) \tag{10}$$

where $\gamma=(y_{\mathrm{c}}-y_1)/D=d_1/D$. Therefore, the total percentage of the vibration energy used for strain sensing is

$$\eta = \eta_1\eta_2 = \frac{(1-\beta)(1-\gamma)}{1/3\alpha^2\beta + 1} \tag{11}$$

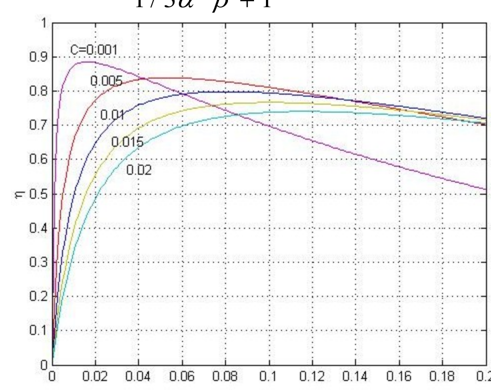

Figure 3. Plot of efficiency η as a function of γ with different C (α =11)[5]

The optimal γ that results in the maximum efficiency is

$$\gamma_O = \frac{1}{1 + \sqrt{1 + \frac{1}{C} + \frac{1+C}{C^2(3\alpha^2+1)}}} \tag{12}$$

where $C = t_1^2/12D^2$ The plot of efficiency η as a function of γ with different C is presented in Fig. 3 [5]. Once γ_0 has been decided, we can easily find the distance between neutral plane and top piezoresistive beam d_2, and other related parameters such as w_1, w_2 and t_2.

In conventional piezoelectric cantilever, there is typically 30-40% of the total mechanical energy stored in the piezoelectric layer in the form of normal strain, contributing to the output signal. In comparison, the asymmetrical gapped cantilever allows 87% or even higher percentage of the mechanical energy to be used for piezoelectric sensing.

III. SENSOR CHARACTERIZATION AND PRELIMINARY TEST

A. Sensor Characterization

A prototype of the piezoelectric accelerometer with a resonant frequency of 1100 Hz and a total weight of 5 gram has been designed and constructed. The size of the prototype sensor is $35mm \times 18mm \times 7.8m$ ($l \times w \times t$) as shown in Fig. 4. A built-in charge amplifier is used to amplify the output voltage of the sensor. Fig. 5 plots the frequency response of the accelerometer characterized on a mechanical shaker. A resonant frequency of 1100 Hz and an average sensitivity of 86V/g in the low frequency band are observed. Fig. 6 shows the noise floor of the sensor characterized in an acoustic isolation room. A noise floor of 40ng/√Hz is observed above 100 Hz. Note that at low frequency, the acoustic noise from environment cannot be completely removed. The actual noise of the sensor is much smaller at low frequency.

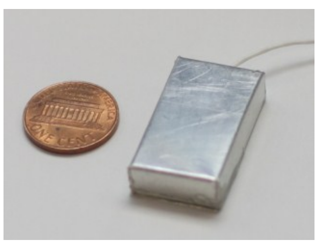

Figure.4 The prototype sensor.

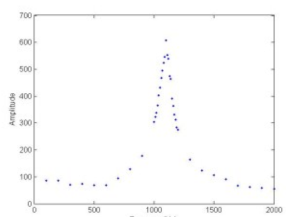

Figure 5. Frequency response of the prototype accelerometer.

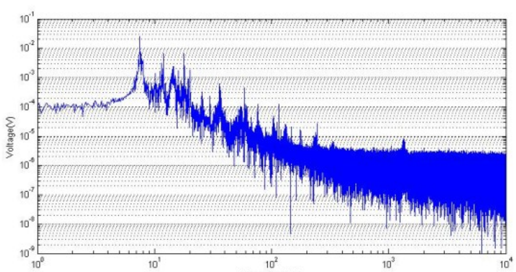

Figure 6. Noise spectrum of the prototype accelerometer

B. Preliminary Tests

Preliminarily tests for recording both heart and lung sounds are carried out on healthy volunteers in a regular laboratory environment. The data from the sensor is transferred to a PC through data acquisition board (NI USB 6210) and further processed by LabVIEW® and MATLAB®. The sampling rate is fixed to be 20 kHz. A comparison is made between the asymmetrical gapped accelerometer and a high-end electronic stethoscope (3M Littman 3200) in detecting heart and lung sounds. For both accelerometer and stethoscope data, a filter with a bandwidth from 20 Hz to 500 Hz is applied to extract the heart sound and a filter with a bandwidth from 350 Hz to 1000 Hz is applied to extract the lung sound. The device location is chosen to be the 5th intercostal space to the left just lateral to the sternum (right AV auscultation) for cardiac signal detection and a right anterior intercostal space above the level of the 3rd rib for respiratory signal detection.

Figure 7 shows the visible differences in signal quality between the asymmetrical gapped accelerometer and the electronic stethoscope in cardiac sound detection. The signal-to-noise ratio of the new sensor is about two times higher. Fig. 8 plots the lung sounds recorded by our sensor and the electronic stethoscope for regular gentle breathing. Note that lung sounds are much weaker than heart sounds and thus are more difficult to detect, especially for a gentle breathing. As can be observed in Fig. 8 (b), the lung sound can hardly be distinguished in the signals captured by the stethoscope. In comparison, the lung sound can be clearly detected by our sensor. It is also worth noting that these measurements were carried out in a regular laboratory environment full of air-borne noises. It can be observed that our sensor is not very sensitive to air-borne noise.

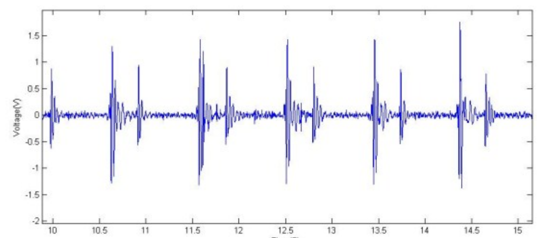

(a)

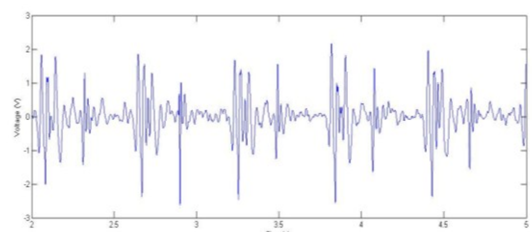

(b)

Figure 7. Sample waveforms of heart sound: (a) detected by our new accelerometer; (b) detected by an electronic stethoscope.

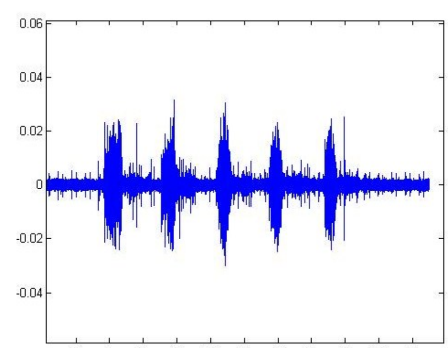

(a)

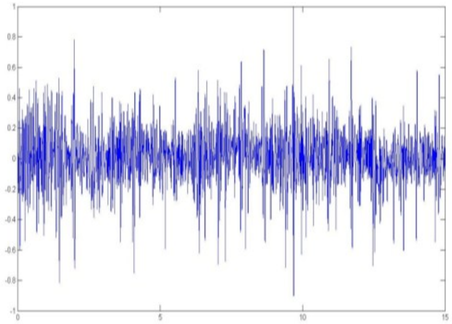

(b)

Figure 8. Sample waveforms of lung sound: (a) detected by our new accelerometer; (b) detected by an electronic stethoscope

IV. Discussion and Conclusion

In summary, the novel accelerometer based on asymmetrical gapped cantilever has the following highly desirable advantages for mobile healthcare: (1) very sensitive, which helps to improve the signal fidelity and capture critical subtle signals which are hard to detect by current acoustic sensors; (2) wearable, which enables long-term continuous monitoring of physiological vital signs; (3) low cost – $20 when mass-produced; and (4) a very robust way of capturing heart/lung sounds – the patients can reliably obtain the same high quality signals as the trained medical personnel.

The new wearable sensor will enable many important clinical applications. The first application can be heart failure (HF) monitoring. For HF management, it is well known that a single parameter or a single symptom is inaccurate and ineffective. Our sensor can provide continuous monitoring of both heart & lung sounds. From the heard sounds, important information for heart failure such as heart rate can be extracted. In addition, abnormal heart sounds, such as the third heart sound (S3), forth heart sound (S4) and systolic murmur, provide valuable information of the heart pathological conditions [8, 9]. It is also possible to measure blood pressure, a critical parameter, from heart sounds indirectly [10, 11]. To provide more comprehensive heart failure monitoring, pulmonary conditions, such as shortness of breath, rales, dyspnea at rest and paroxysmal nocturnal dyspnea, are of critical importance as well [12]. The new sensor developed will allow us to monitor pulmonary conditions continuously by detecting the lung sounds on the chest. Note this has not been possible before since the lung sounds are much weaker than heart sounds and thus are more difficult to detect, especially in a mobile setting. Note that the noise caused by patient movement can be a potential obstacle for these applications. We are currently investigating a number of approaches to address this issue.

Acknowledgment

The authors thank Hongen Tu and Eric Kim for their help in the development and characterization of the sensor.

References

[1] V. Padmanabhan, J. L. Semmlow, and W. Welkowitz, "Accelerometer type cardiac transducer for detection of low-level heart sounds," *IEEE Transactions on Biomedical Engineering,* vol. 40, pp. 21-28, Jan 1993.

[2] K. J. Cho and H. H. Asada, "Wireless, battery-less stethoscope for wearable health monitoring," in *IEEE 28th Annual Northeast Bioengineering Conference, April 20, 2002 - April 21, 2002*, Philadelphia, PA, United states, 2002, pp. 187-188.

[3] S. Henneberg, B. Hoк, L. Wiklund, and G. Sjodin, "Remote auscultatory patient monitoring during magnetic resonance imaging," *Journal of clinical monitoring,* vol. 8, pp. 37-43, Jan 1992.

[4] Q. L. Zheng and Y. Xu, "Asymmetric air-spaced cantilevers for vibration energy harvesting," *Smart Materials & Structures,* vol. 17, Oct 2008.

[5] Y. F. Li, Q. L. Zheng, Y. T. Hu, and Y. Xu, "Micromachined Piezoresistive Accelerometers Based on an Asymmetrically Gapped Cantilever," *Journal of Microelectromechanical Systems,* vol. 20, pp. 83-94, Feb 2011.

[6] Q. Zheng and Y. Xu, "Vibration energy harvesting device based on asymmetric air-spaced cantilevers for tire pressure monitoring system," in PowerMEMS Workshp, Washington DC, USA, December 1-4, 2009.

[7] M. H. Bao, *Micro Mechanical Transducers: Pressure Sensors, Accelerometers and Gyroscopes*: Elsevier Science, 2000.

[8] S. Khoor, I. Kovacs, K. Fugedi, G. Horvath, E. Domijan, and M. Domijan, "Telemedicine digital phonocardiography: Cost-effective strategies in heart failure screening and monitoring," in *Computers in Cardiology 2007, CAR 2007, September 30, 2007 - October 3, 2007*, Durham, NC, pp. 649-652.

[9] M. E. Tavel, "Cardiac auscultation - A glorious past - And it does have a future!," *Circulation,* vol. 113, pp. 1255-1259, Mar 7 2006.

[10] J. Xu, L. G. Durand, and P. Pibarot, "A new, simple, and accurate method for non-invasive estimation of pulmonary arterial pressure," *Heart,* vol. 88, pp. 76-80, Jul 2002.

[11] X. Y. Zhang, E. MacPherson, and Y. T. Hang, "Relations between the timing of the second heart sound and aortic blood pressure," *IEEE Transactions on Biomedical Engineering,* vol. 55, pp. 1291-1297, Apr 2008.

[12] A. L. Bui and G. C. Fonarow, "Home Monitoring for Heart Failure Management," *Journal of the American College of Cardiology,* vol. 59, pp. 97-104, Jan 2012.